Observational needs for understanding solar magnetic activity and the formation of large-scale transient events

Lidia VAN DRIEL-GESZTELYI[1,2,3]

(1) UCL/MSSL, UK (2) Paris Observatory, France (3) Konkoly Observatory, Hungary

Coimbra Solar Physics Meeting, 2015

Secchi

CME during an eclipse – 18 July 1860

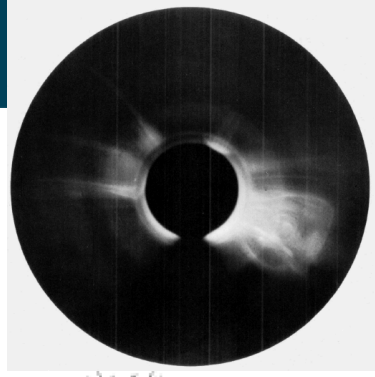

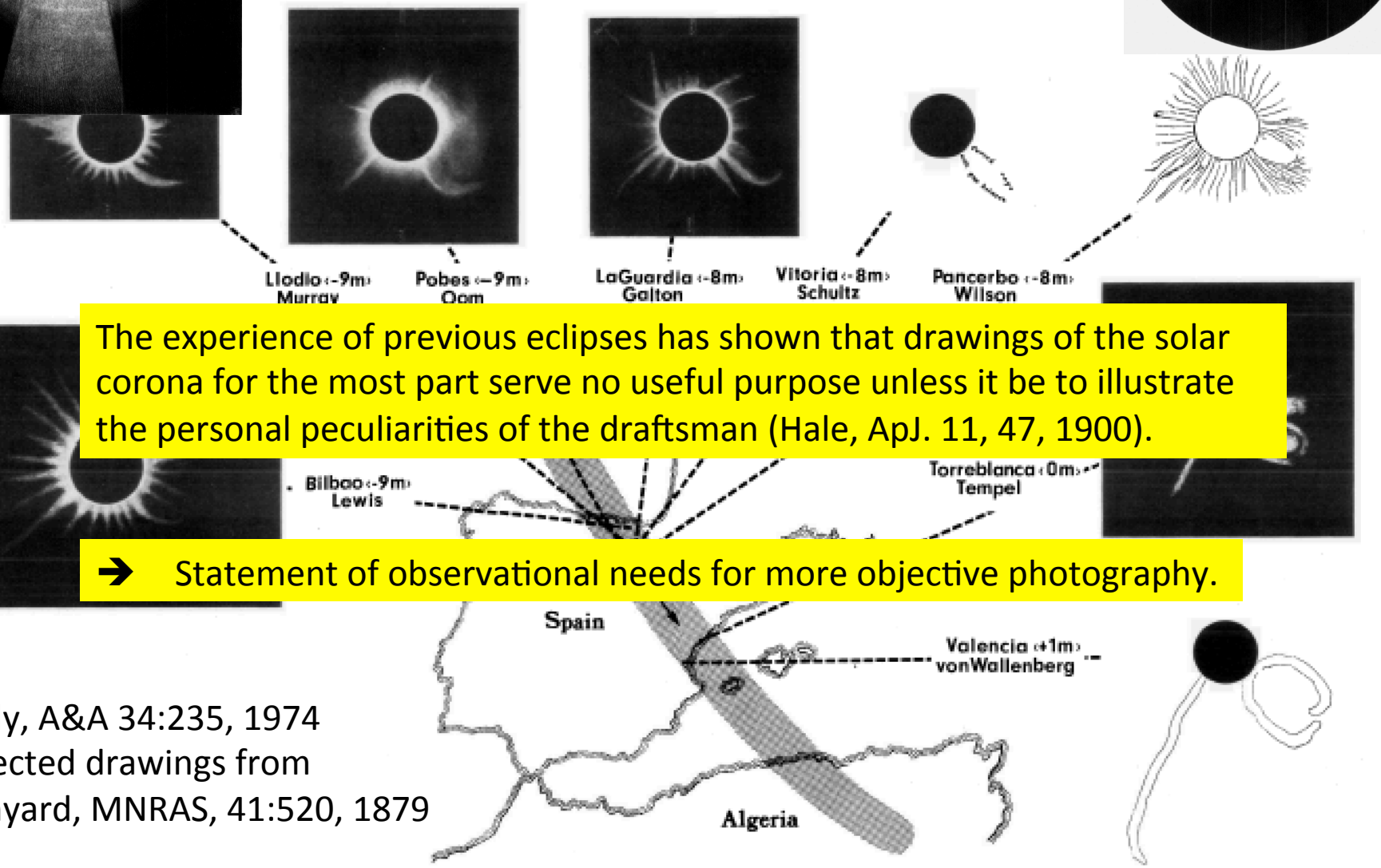

The experience of previous eclipses has shown that drawings of the solar corona for the most part serve no useful purpose unless it be to illustrate the personal peculiarities of the draftsman (Hale, ApJ. 11, 47, 1900).

➔ Statement of observational needs for more objective photography.

Eddy, A&A 34:235, 1974
Selected drawings from
Ranyard, MNRAS, 41:520, 1879

CSHKP model for eruptive solar flares (CMEs)

(Carmichael 1964; Sturrock 1966; Hirayama 1974; Kopp & Pneuman 1976)

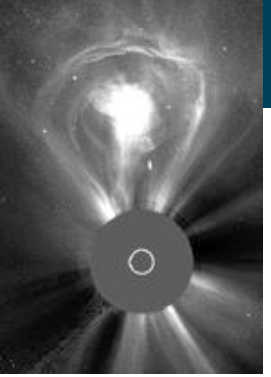

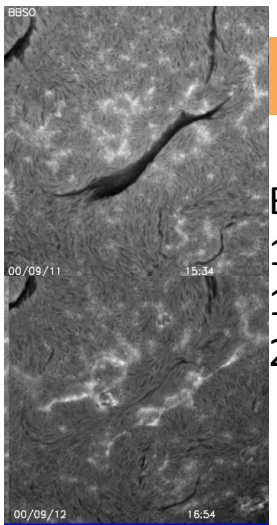

BBSO
11/09
12/09
2000

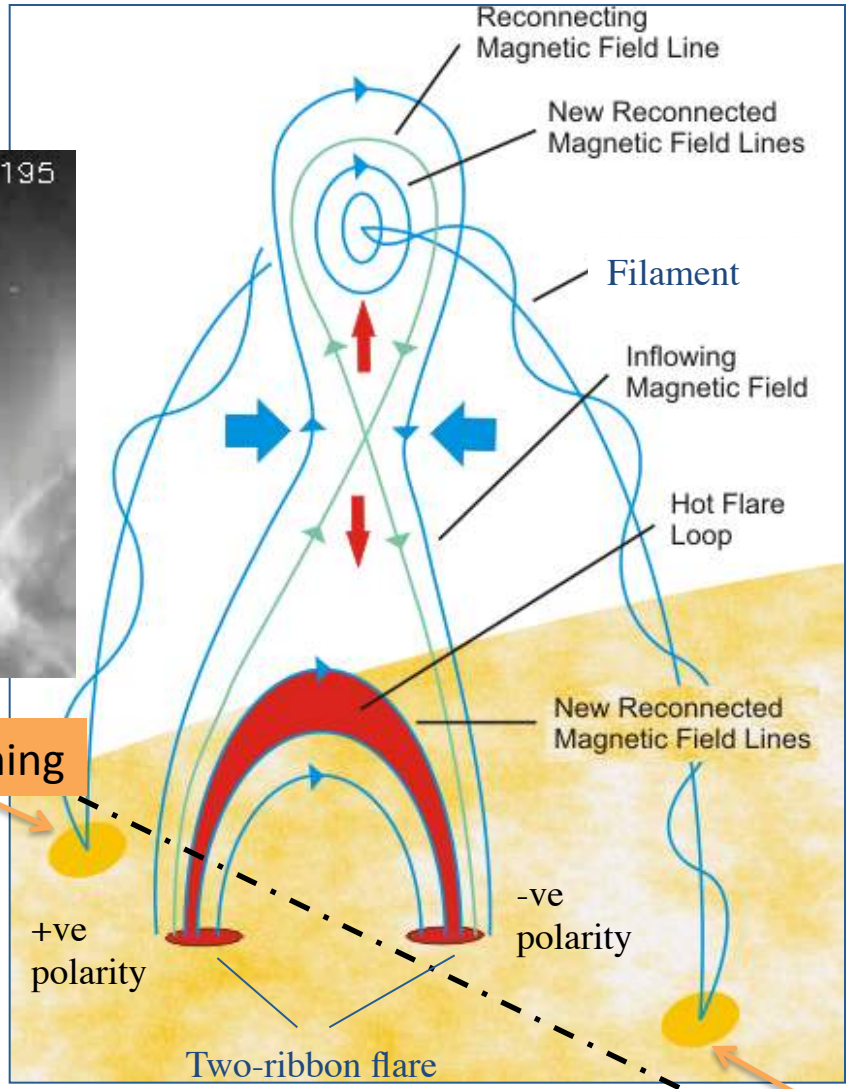

Dimming

Dimming

Adapted from Shibata (1998)

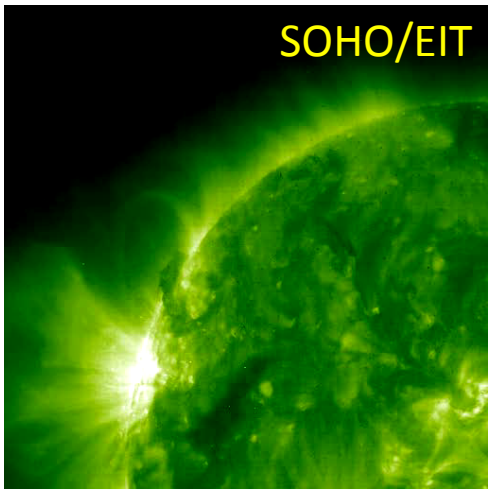

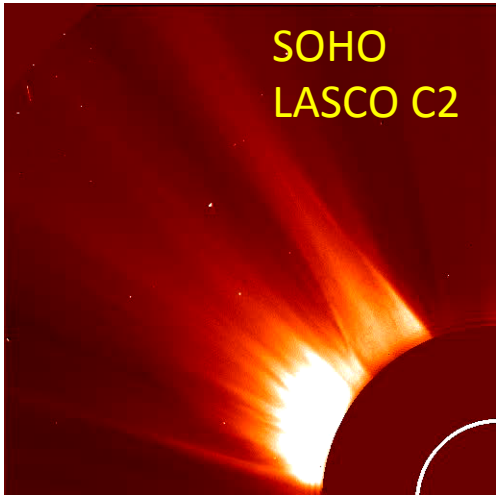

How CMEs form? - Models

Pre-eruption configuration: Stressed core field + stabilising overlying field

Flux rope

Sheared arcade

Evolution leading to eruption

Emerging flux

Flux cancellation

Twisting

Shearing

Onset

Kink instability

Breakout

Driver

Torus instability

As the sheared arcade is converted into a flux rope during the eruption, all CME models at some stage will have a flux rope; CMEs are increasingly modeled as erupting flux ropes.

All models produce a current sheet under the erupting flux rope, and a flare.

A long list of references from Antiochos et al. (1999) to Török and Kliem (2005, 2007)… Quanhao Zhang et al. 2014, Kliem, Lin, Forbes, Priest & Török, ApJ, 2014; Seaton et al., 2011; Keppens et al., 2014…

How CMEs form and evolve? - Observations

Evolution leading to eruption	Synoptic magnetic field observations, WL, chromospheric lines (Hα), expansion (EUV spectroscopy) , sigmoid formation (EUV), radio…
Onset	Slow rise filament (Hα, UV), SXR, radio bursts
Impulsive & post-impulsive phases	Flare (all wavelengths, including particle detectors), fast rise filament (Hα, UV), 3-part structure (coronagraphs)
Lower-coronal effects	Global wave (Hα-EUV-radio), dimming (EUV), restructuring (EUV, radio)
Propagation	Coronagraphs, heliospheric imagers, in-situ measurements, radio scintillation, hm-km radio, particle detectors (shock)

All the wavelengths provide complementary information, they have to be used in combination. Observations should be combined with modeling to help with their interpretation.

Build-up phase: Flux cancellation – fluxrope formation

AR 10977

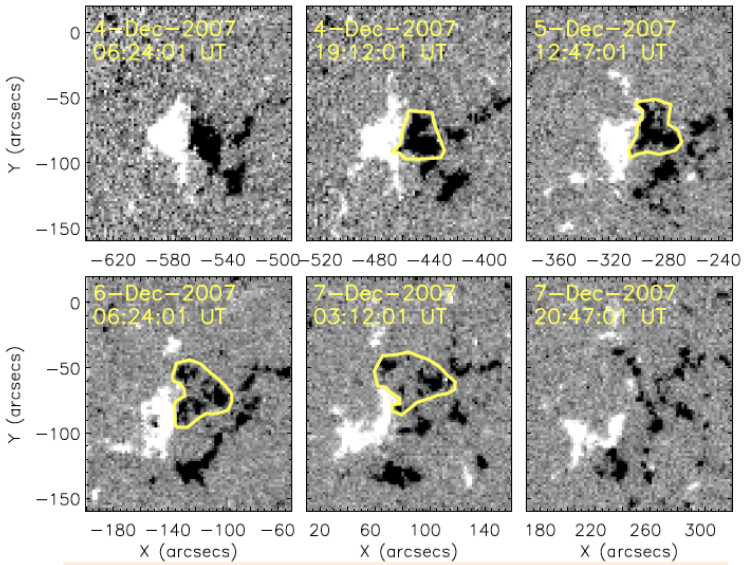

34% of the peak AR flux cancels 2.5 days prior to the eruption.

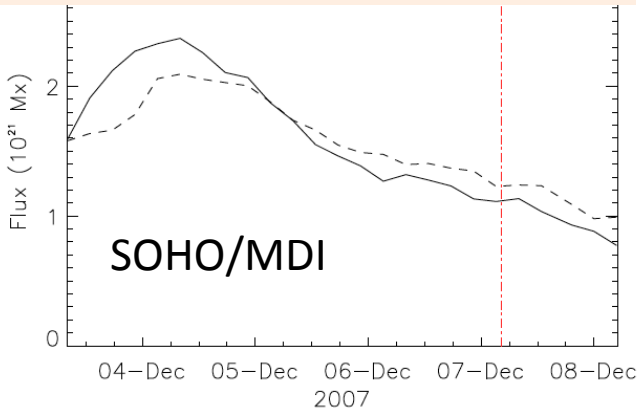

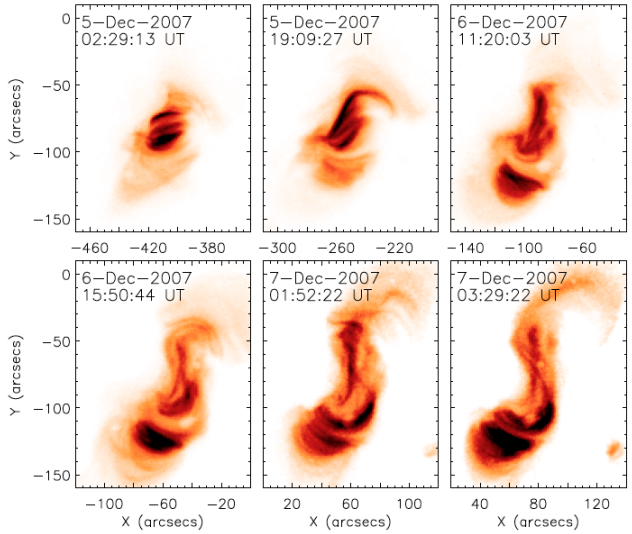

Hinode/XRT

Green et al. (A&A, 526, A2, 2011)

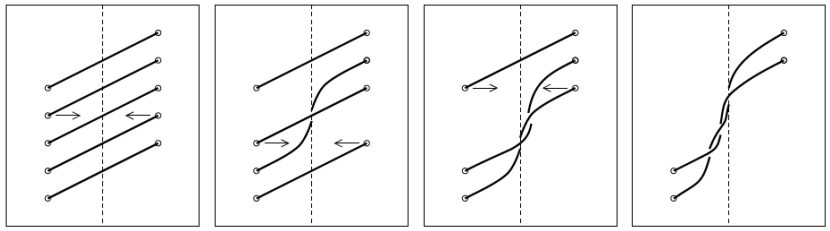

2/5 of flux: fluxrope,
3/5 of flux: cancels

Modelling: Poloidal and axial flux in **the flux ropes** for most models amounts to about **60-70% of the cancelled flux** and **30-50% of the total flux** in the regions. (Savcheva et al., ApJ 759, 105, 2012)

Evidence for bald patch topology in a pre-eruption sigmoid

17 October 2007 Hinode XRT

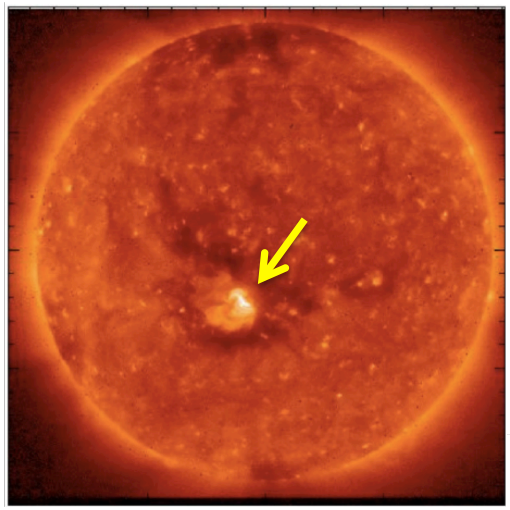

FIP bias map Hinode/EIS

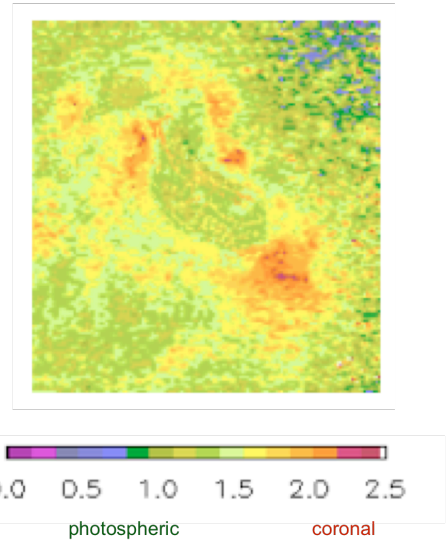

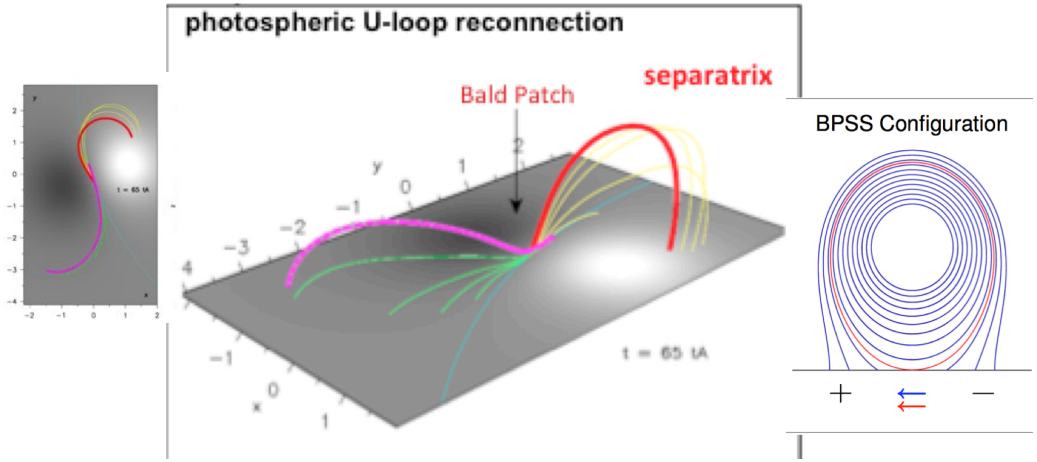

Aulanier et al., ApJ, 708:314, 2010

Reconnection that builds the flux rope occurs in the lower part of the solar atmosphere and inputs photospheric plasma in upwardly curved field lines (bald patch)

Evidence from coronal abundances: Photospheric FIP bias along the inversion line in a sigmoid.
Low/High FIP: Mg, Si, Fe/C, O, Ne, S
Division at ~10 eV.

Baker et al, ApJ 778:69, 2013

Spectroscopic signature of flux rope expansion pre-eruption

17 Oct. 2007

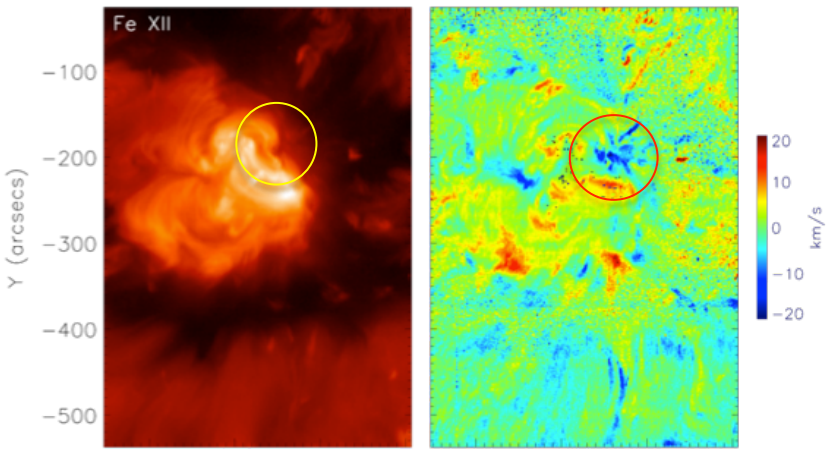

18 Oct. 2007 – CME -6 hrs

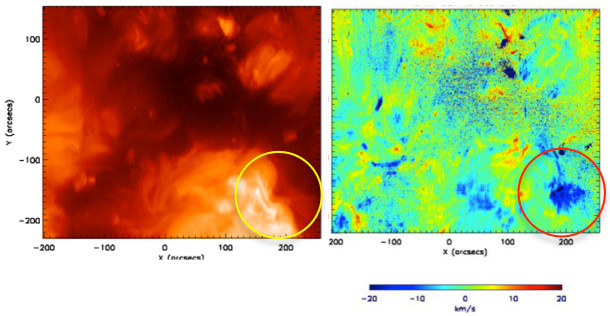

eruption

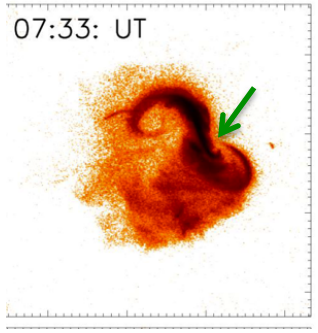

CME started on 18 Oct. at ≈07:30 UT

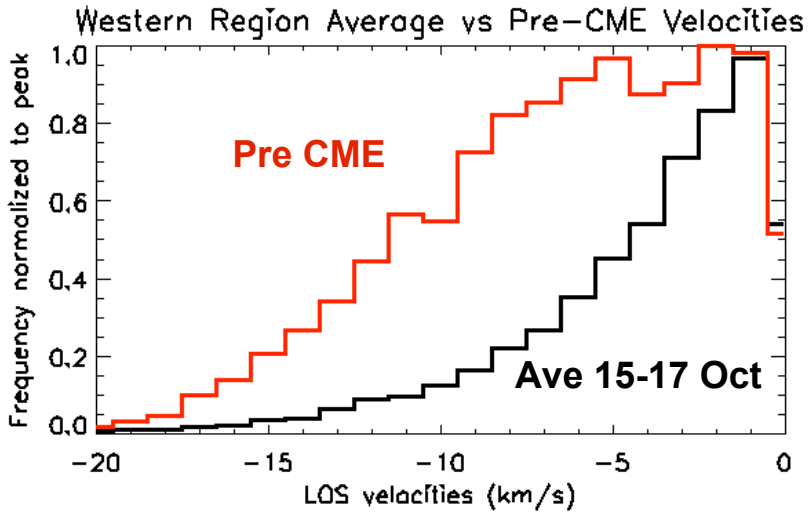

Slow expansion of the **flux rope** prior to the CME eruption **led to stronger compression** of the surrounding field and **intensification** of **outflows** on the western side of the AR.

Baker et al., Solar Phys 276, 219, 2012.

CME initiation by sunspot rotation – data-constrained simulations of the 6 July 2006 event

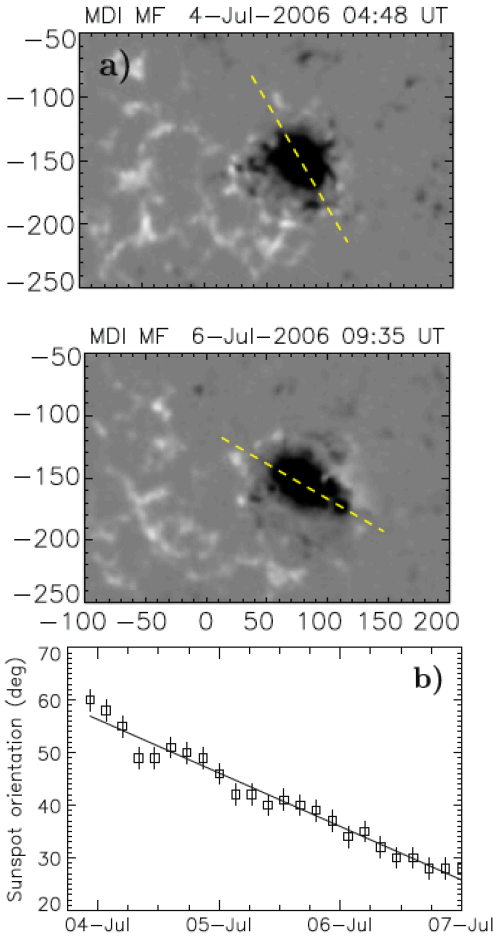

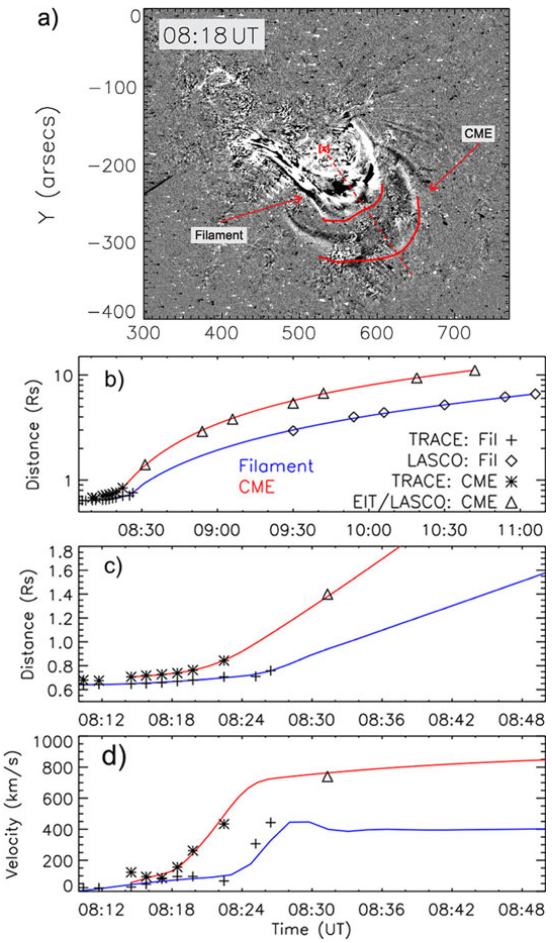

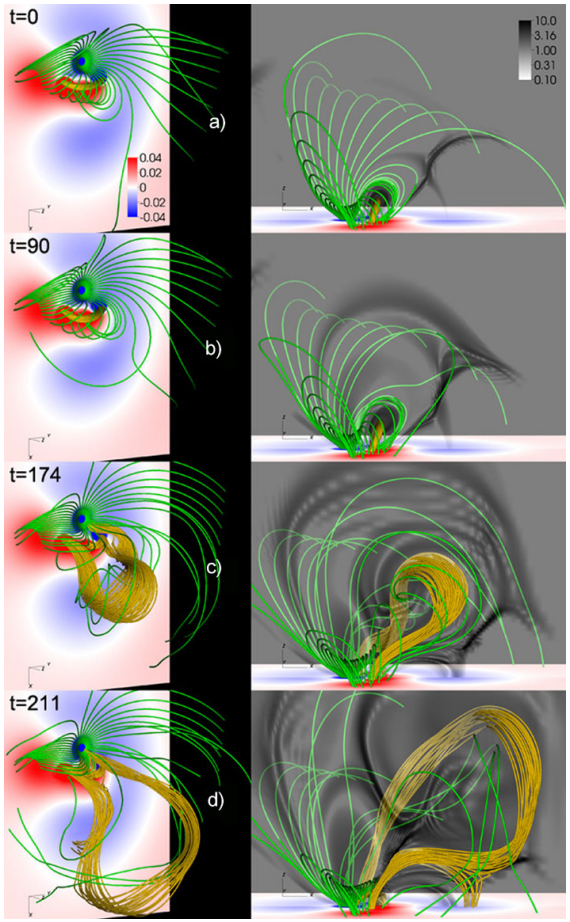

The **rotation** triggered the eruption by **progressively expanding the magnetic field** above the filament.

Török et al., Solar Phys. 286:453, 2013

Helix (flux rope) in a CME core

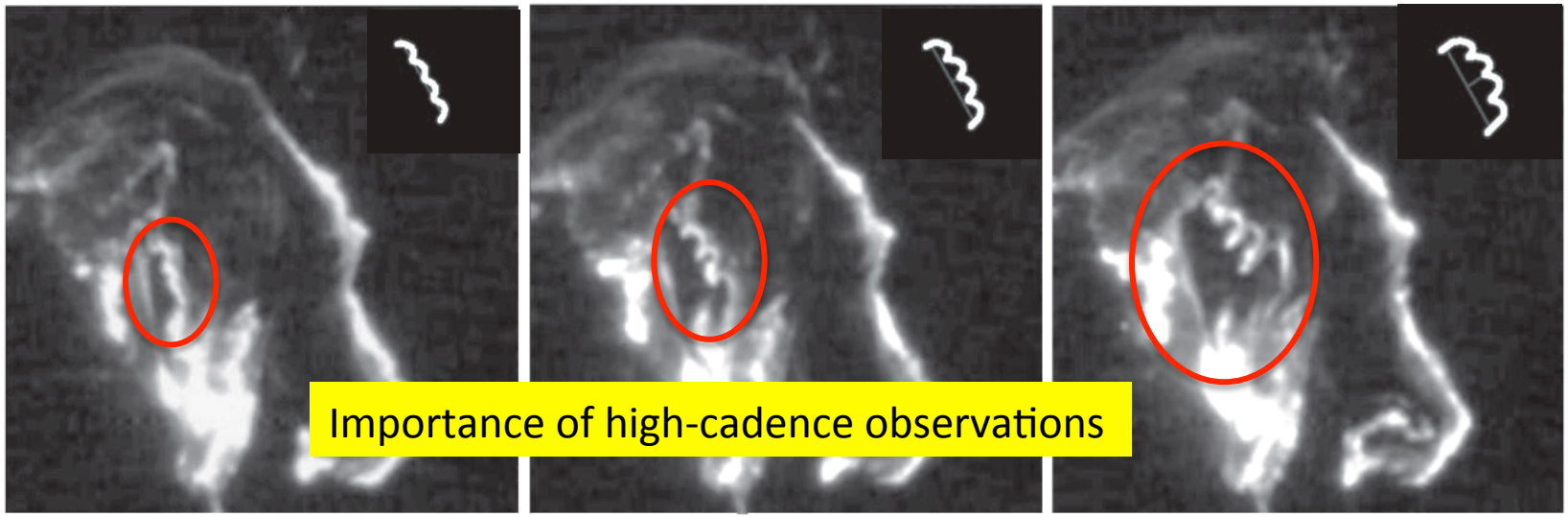

- Gary and Moore (ApJ 611:545, 2004) C IV, TRACE 160 nm (UV) images of the 15 July 2002 CME.
- The base length of the helix is 39 Mm.
- Twisted structure is also visible in the resulting CME.
- Extreme example of twist in an eruption. It is also easy to miss (it was visible for 28 sec only).

Kink and torus instabilities in action

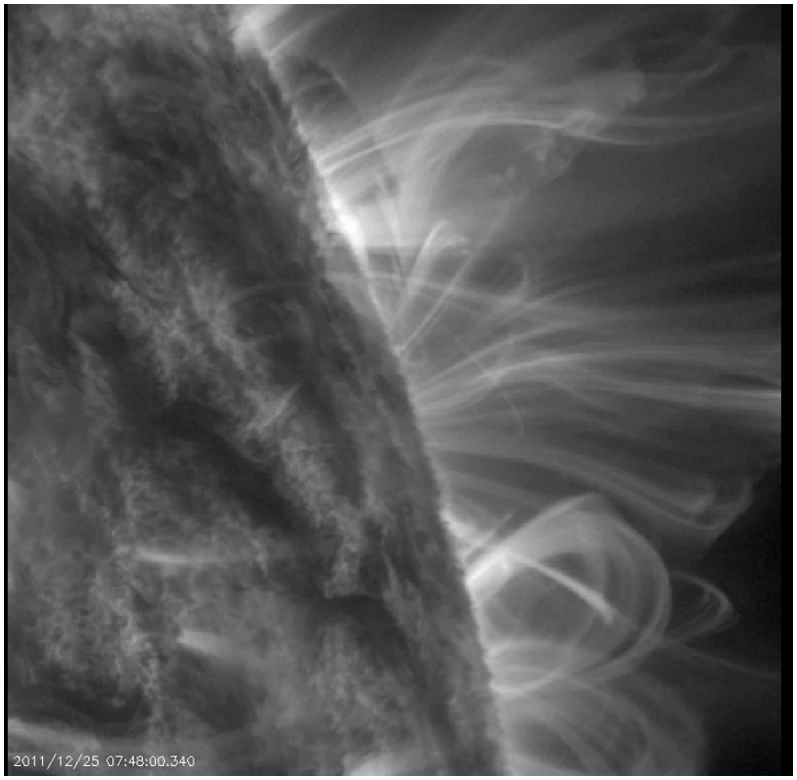

SDO/AIA 171 A movie
25 Dec. 2011 07:48-08:53 UT
Courtesy Angelos Vourlidas

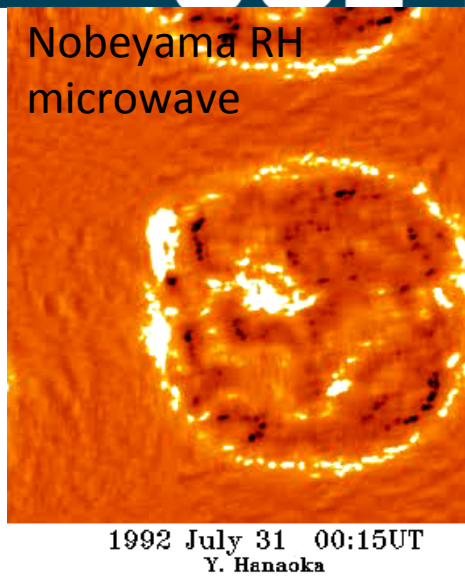

Slow rise of the filament

Kink instability:
>3π, twist profile and aspect ratio dependent

Torus instability: (a) driven by the hoop force (gradient of the magnetic pressure $p_m=B^2/2\mu_0$) in a semi-circular flux rope
(b) Occurs when the decrease of downward magnetic tension with increasing altitude (decay index) becomes faster then the upward magnetic pressure gradient (Török and Kliem, 2007)
Decay index represents the potential **magnetic field drop-off along the vertical direction** (z-axis): $n = -d \ln B / d \ln z$.

Erupting filament, cavity, current sheet

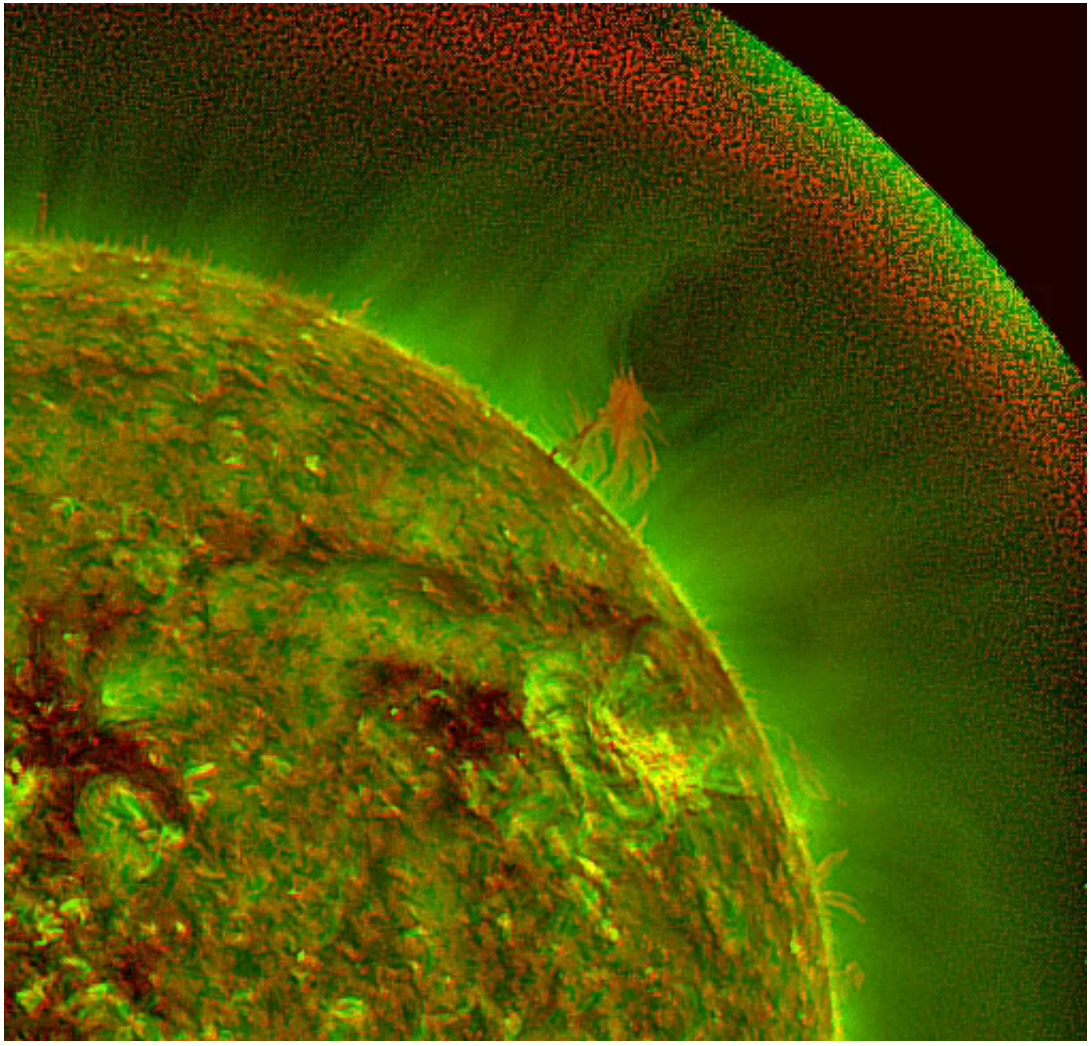

- Cool dense filament material is carried away from the Sun by the erupting magnetic flux rope in the dips of the helical field lines.
- Current sheet forms under the departed flux rope.

Importance of co-aligned multi-T observations.

SDO/AIA 304 ($5x10^4$) + 193 ($1.2x10^6$ + $2x10^7$) Å movie
13 June 2010 00:00-21:34 UT
Courtesy Angelos Vourlidas

Radio CME – 15 April 2001 X 14 flare/CME

Pre-Event/Initiation

Démoulin et al, ApJ 750:147, 2012

Impulsive phase

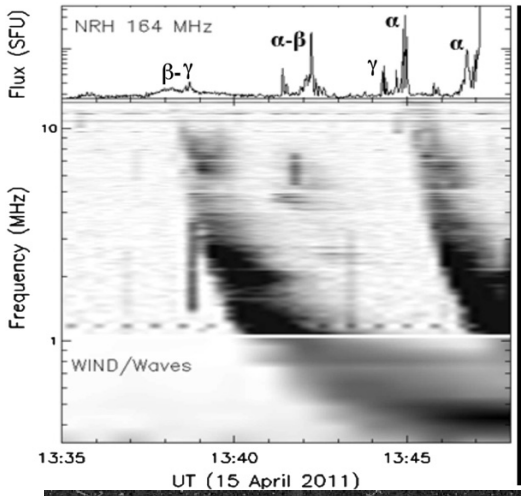

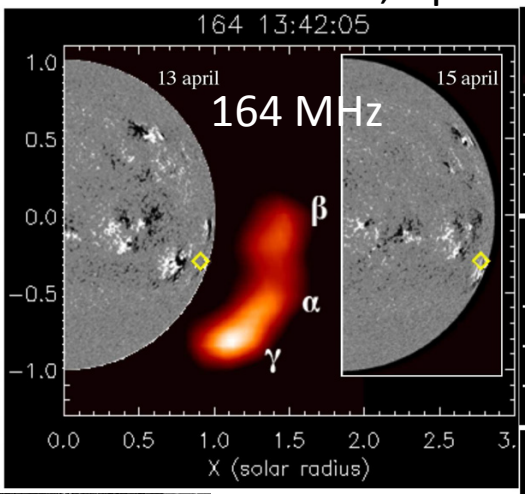

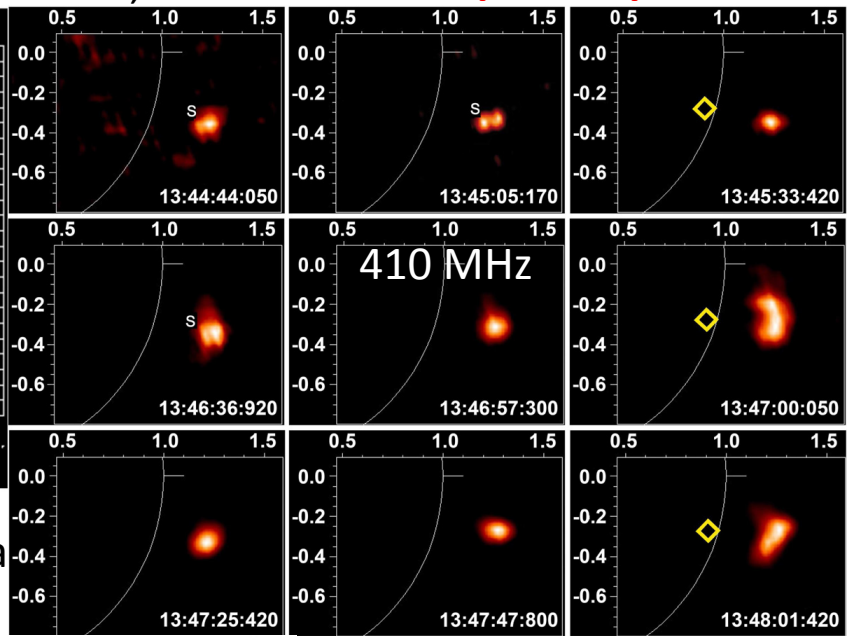

Nançay RH data (metric)

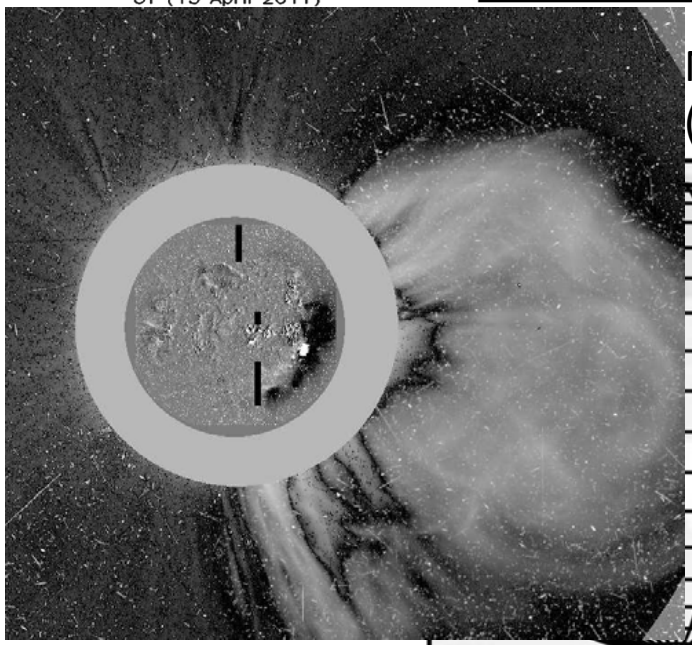

Post-impulsive phase

236 & 164 MHz

(CME + type III)

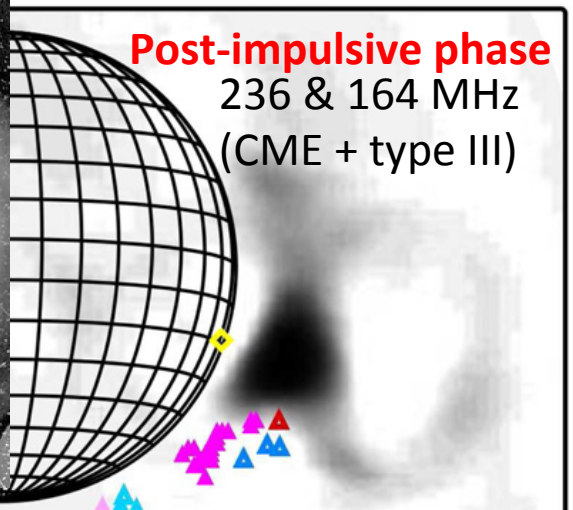

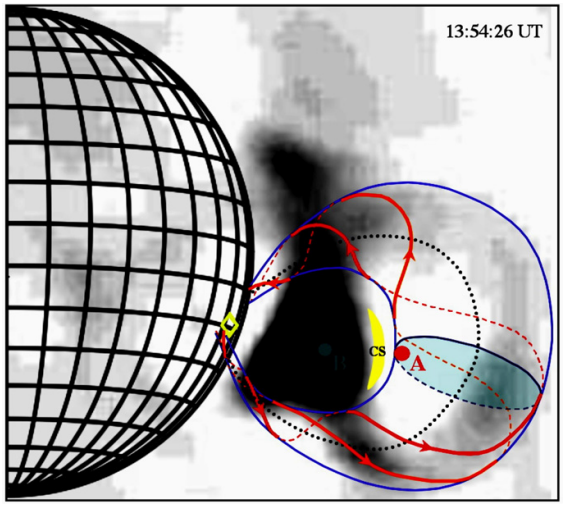

What is a radio-CME and what does it tell us?

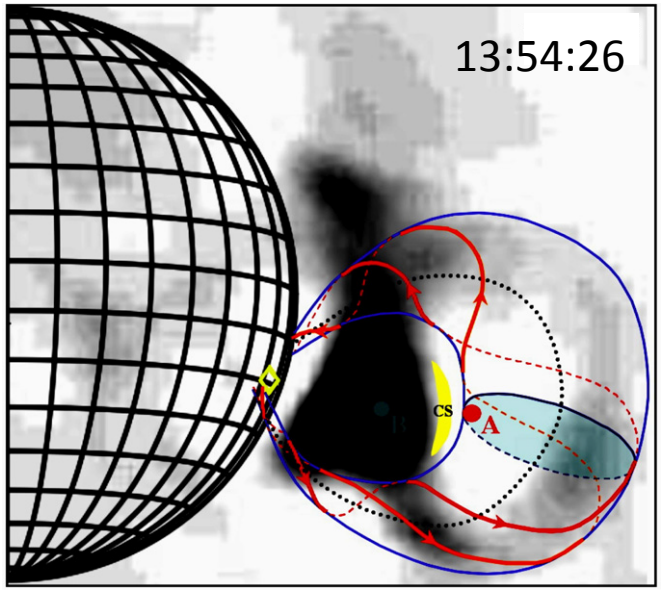

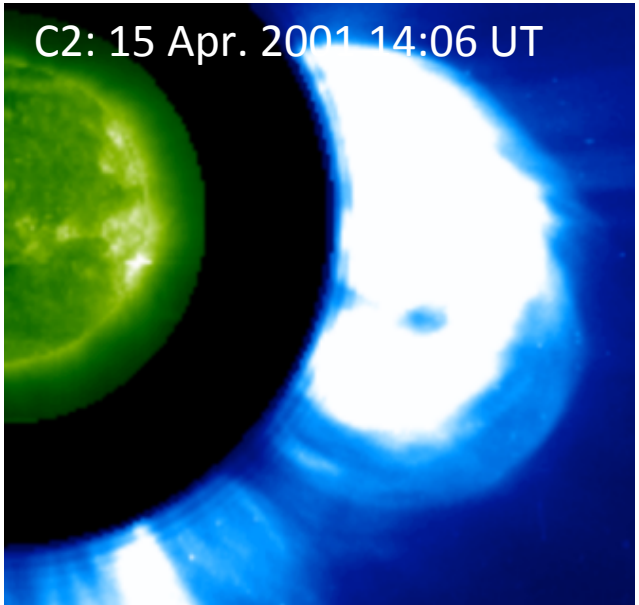

Bastian et al., ApJ 558, 65, 2001
Maia et al., ApJ 660, 874, 2007
Démoulin et al., ApJ 750, 147, 2012

- Radio CME ≅ WL flux rope cavity
- It is illuminated by synchrotron emission from relativistic electrons
- The source of relativistic electrons is bursty reconnection under the erupting flux rope
- The radio CME is smaller than the WL CME, which also contains compressed coronal plasma
- Lateral over-expansion of the CME and its interaction with streamers (pile-up) and surrounding magnetic fields leads to type II and type III bursts

Impulsive phase – supra-arcade downflows

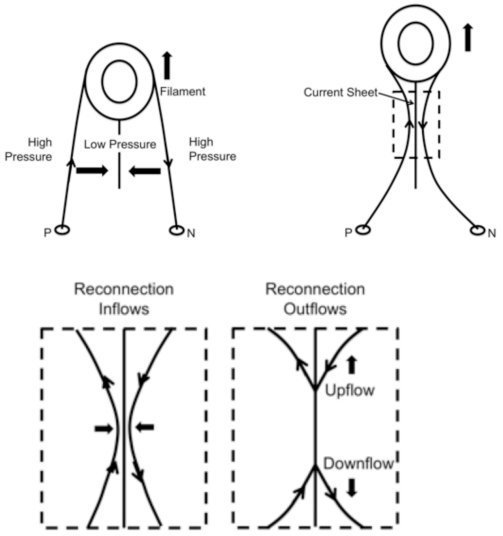

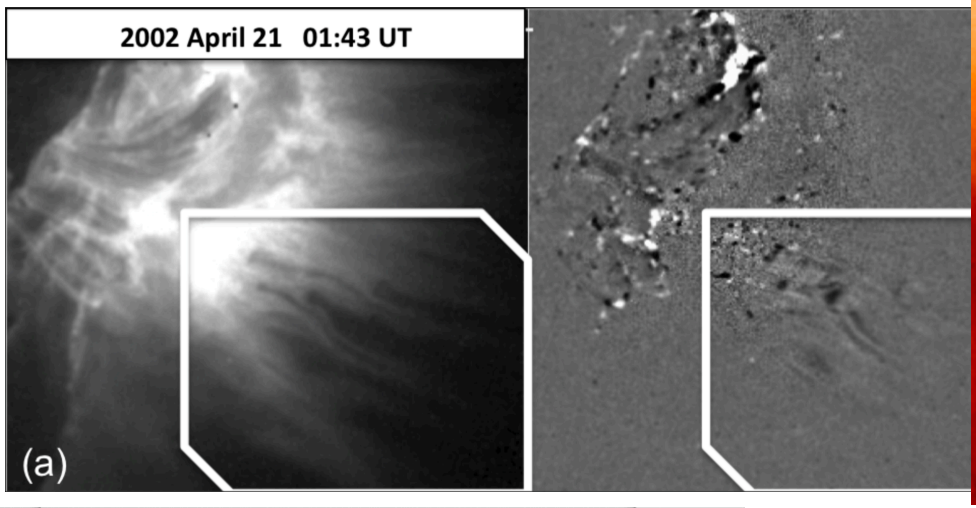

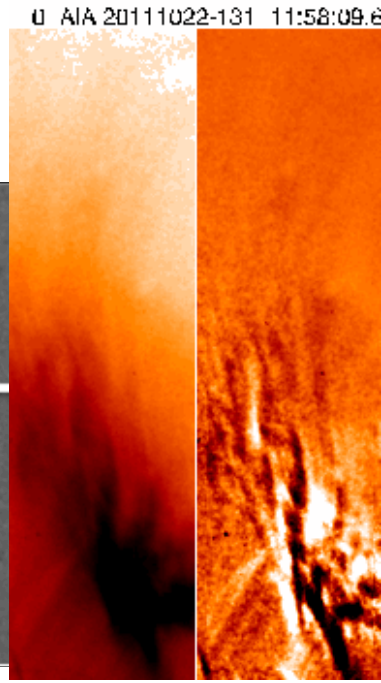

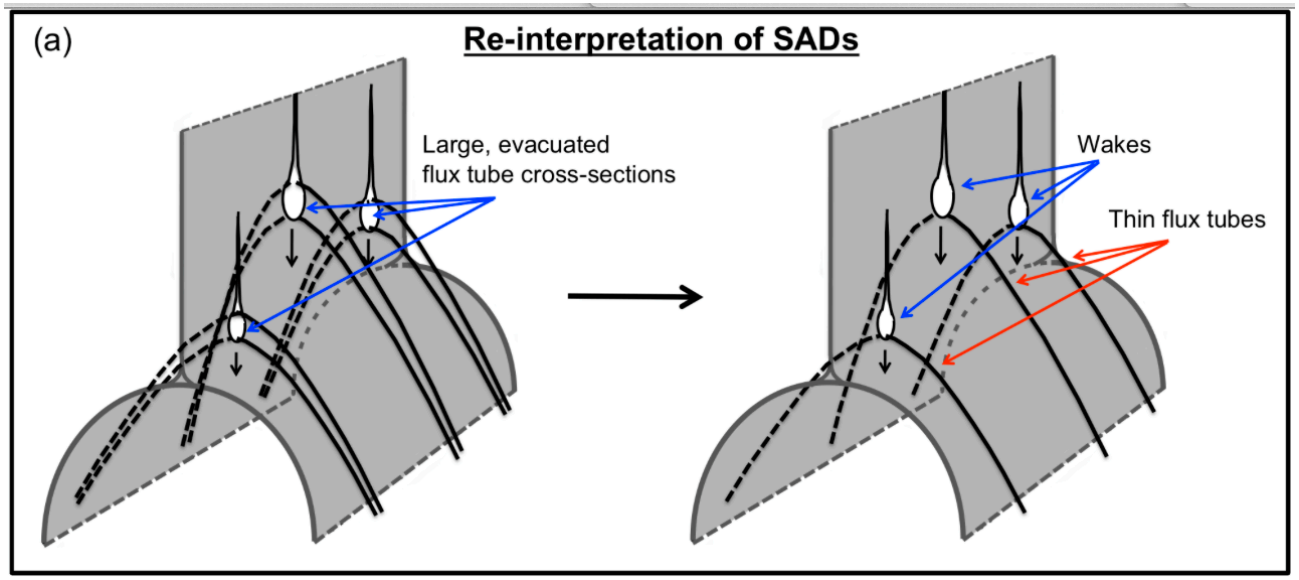

22 October 2011 (SDO/AIA 131). Thin shrinking loops are observed at the leading edge of the voids, revealing SADs to be the wakes created by the passage of the loops through the hot, supra-arcade plasma.

Savage et al. ApJ 747:L40, 2012

Lower-coronal signatures: flare

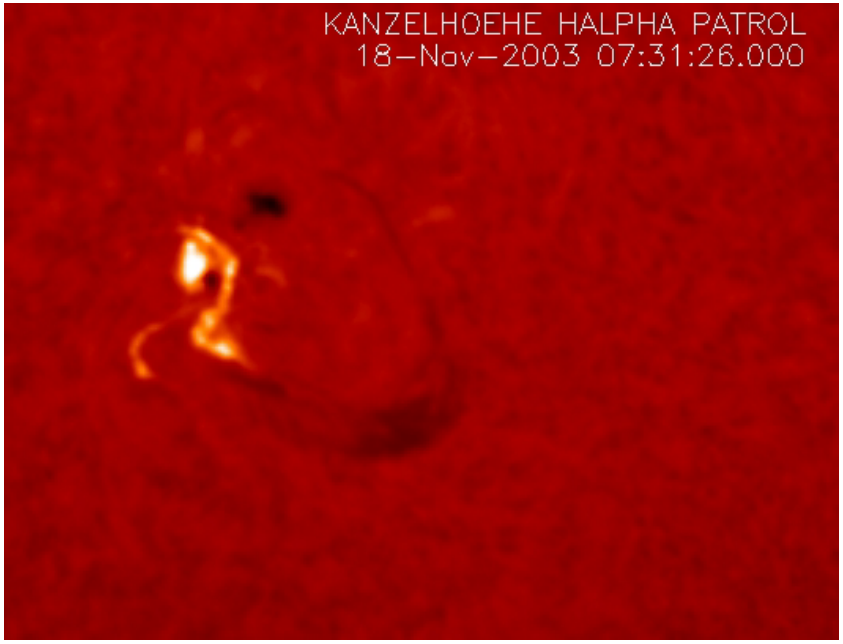

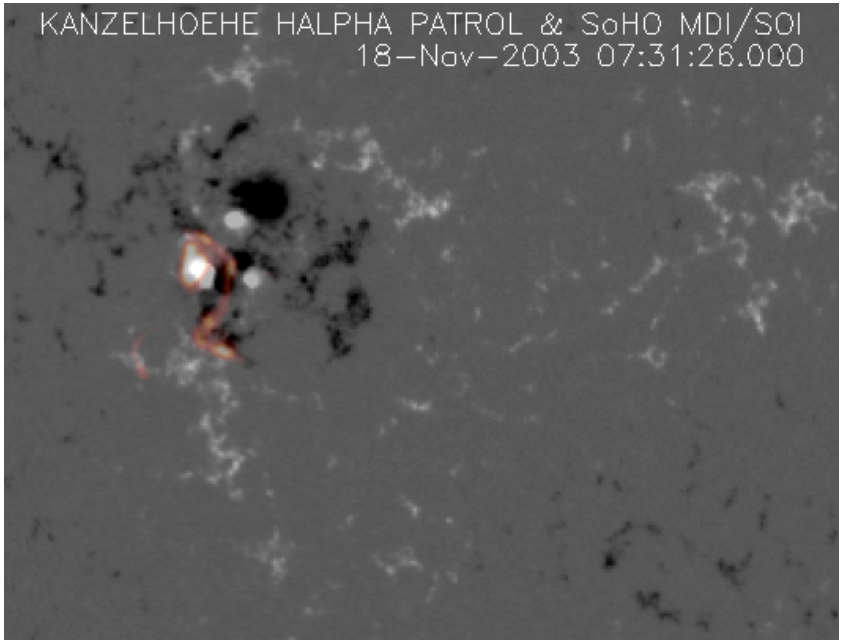

Kanzelhöhe Observatory Hα blue-wing (0.7 Å patrol images and SOHO/MDI magnetograms showing the evolution of the 18 Nov. 2003 filament eruption/flare/CME (M3.9/2N) event.

- Two-ribbon flare with ribbons over opposite polarities.
- Ribbons separate with time

Impulsive phase - flare

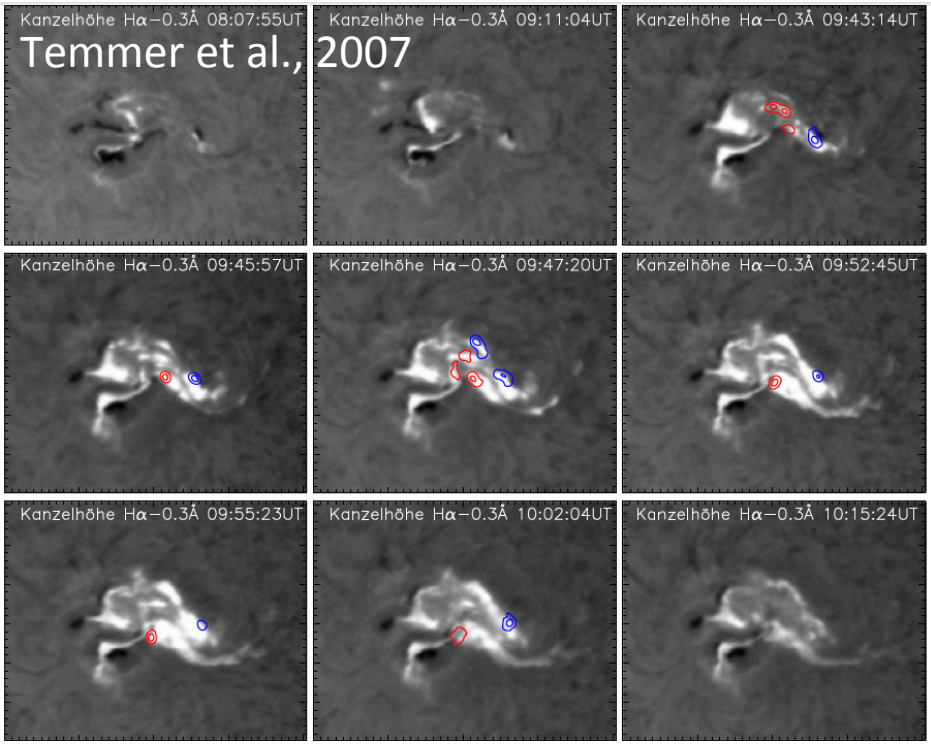

Temmer et al., 2007

Qiu et al., 2007

Fletcher et al., SSRv, 159, 19, 2011

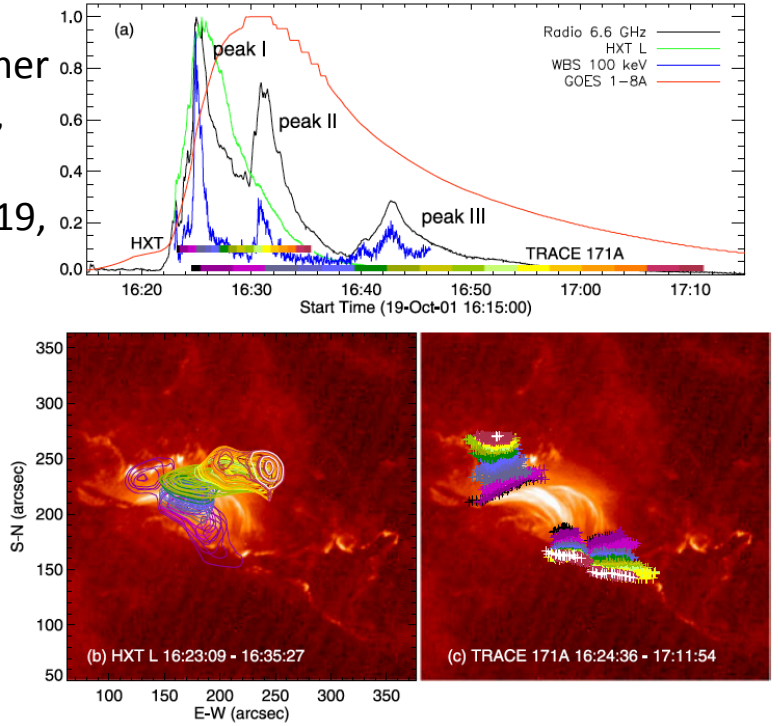

Kanzelhöhe Observatory Hα-0.3 A images of the X3.8 flare/CME on 17 Jan. 2005
Contours: RHESSI 30-100 keV images (red +; blue −)
Tempo

Evolution of the 19 Oct. 2001 X1.6 flare in X-rays, microwave lightcurves (top) (left) 14-23 keV HXR contours
(right) footpoint locations color coded.

Small scales, fast changes – need for high temporal and spatial resolutions.

Downward propagating accelerated particles lose their energy once they impact in denser layers, producing bremstrahlung radiation (HXRs), footpoint heating (ribbons), evaporation fills reconnected loops with hot plasma (flare loops). Ribbons separate, flare loop arcade grows.

Flare-related reconnection – effect on CME propagation

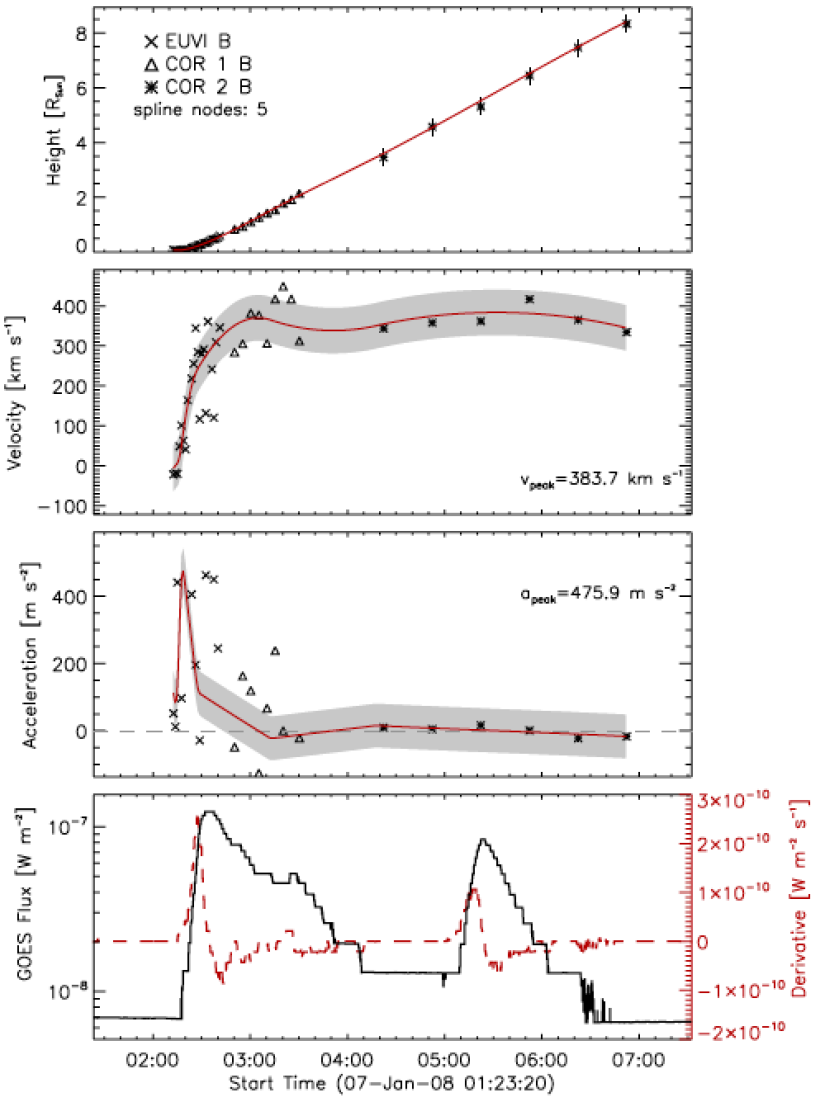

Bein et al., 2012

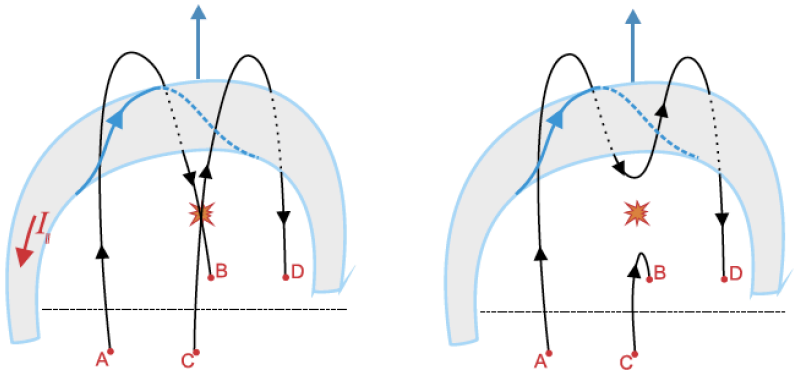

Schmieder et al., Solar Phys. 2015

Flare-related magnetic reconnection under the rising flux rope further increases the poloidal flux of the flux rope, increasing the hoop force driving it upward.

Maximum acceleration is reached
- at a height comparable with the footpoint half-distance (Vršnak, 1990; Chen and Krall, 2003)
- within 1 min of the HXR burst peak or the SXR flux derivative (e.g. Temmer et al., ApJ 712:1410, 2010; Bein et al., ApJ 755, 44, 2012).

Lower-coronal lateral effects: Global coronal waves

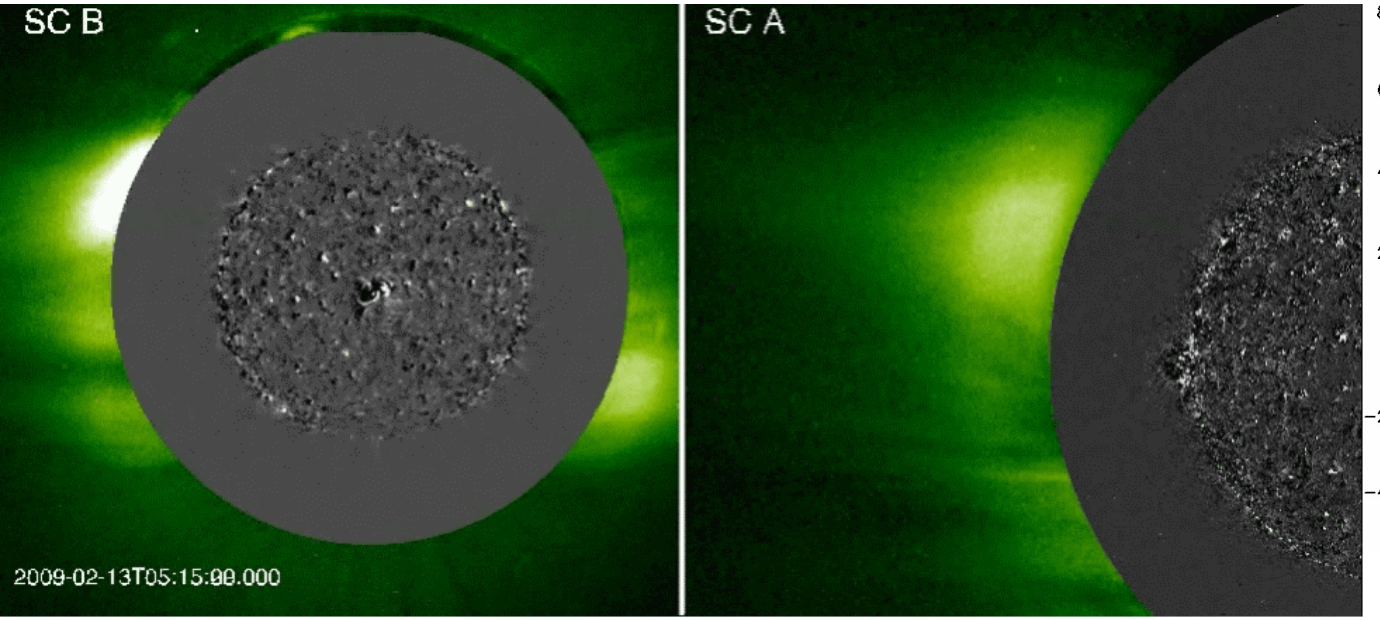

13 Feb. 2009 CME observed by the two STEREO spacecraft in quadrature.

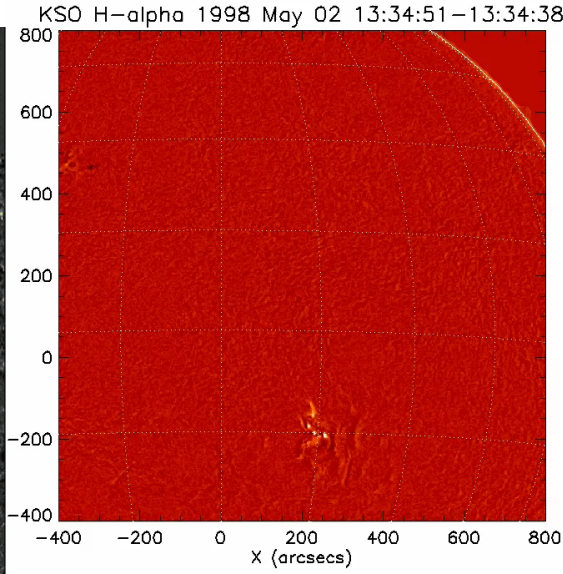

Moreton wave observed at KSO on 2 May 1998 – ground-track of the coronal wave front.

Global coronal waves show multiple wavefronts. A faster wavelike disturbance (a fast-mode MHD wave or shock) is being followed by a slower perturbation that is related to the magnetic reconfiguration of the corona caused by an erupting CME. (Warmuth, LRSP, 2015)
The freely propagating wave is formed by the rapid lateral expansion of the CME in the low corona (Vršnak and Cliver, Solar Phys. 253:215, 2008; Patsourakos et al., ApJ 724:L188, 2010)

Directly observable in EUV, SXRs, chromospheric lines, radio imaging, type II bursts.

Shock-accelerated particles

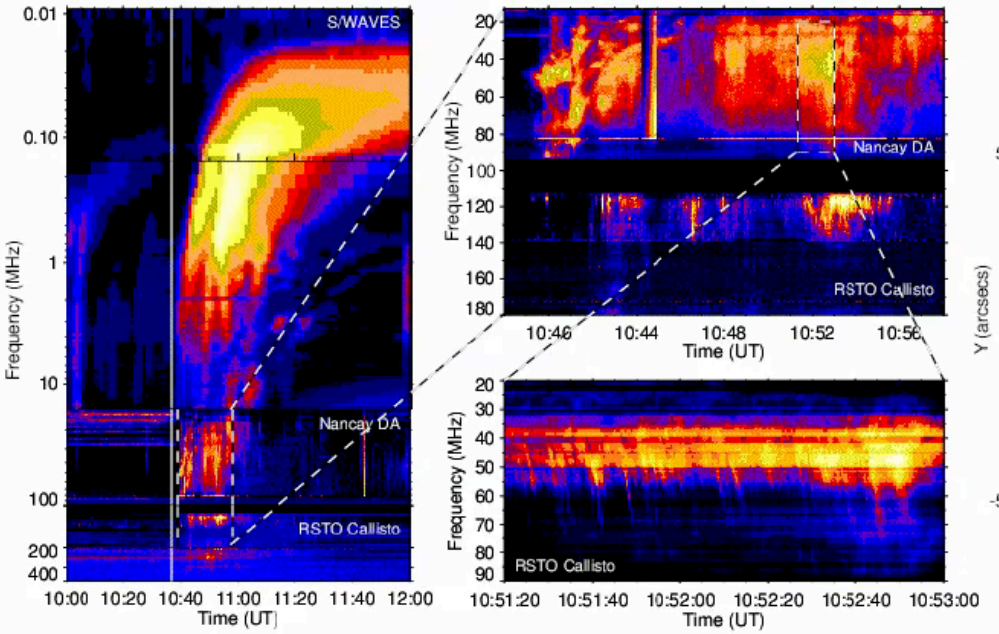

Carley et al., Nature Phys. 2013

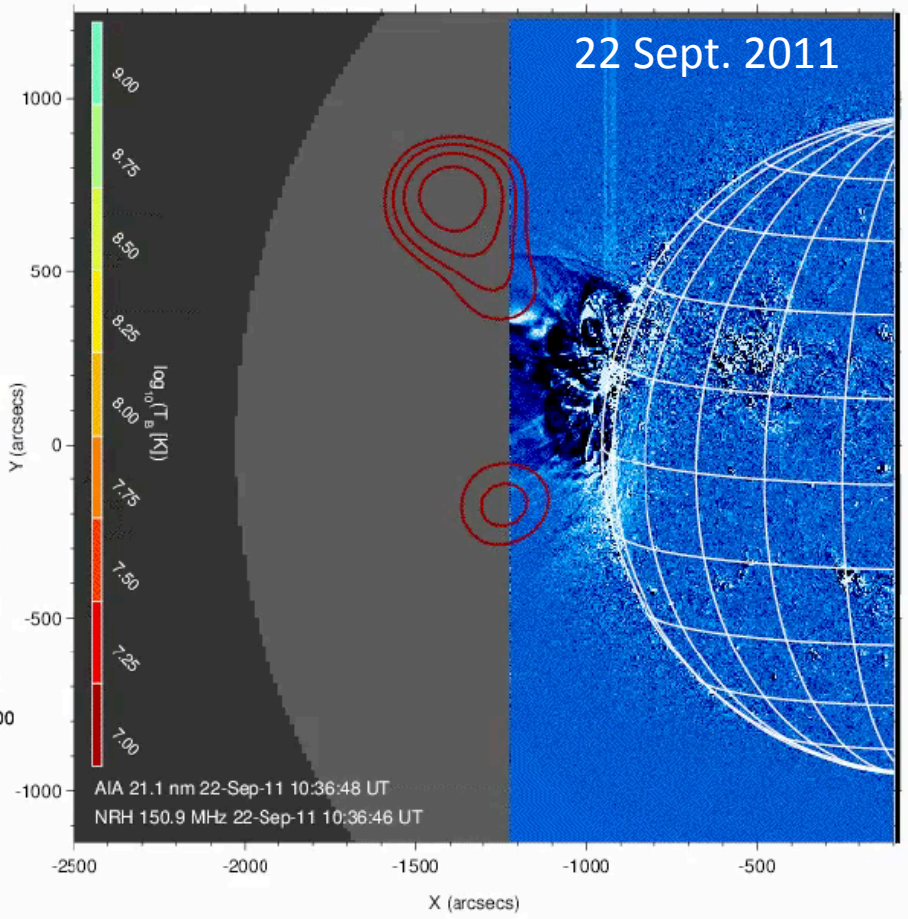

- AIA 21.1 nm & Nançay Radioheliograph 150.9 MHz
- Type II shock emission, Type III particle and herringbone emission.

However, only 54% of 138 SDO-era global waves were accompanied by Type II bursts (Nitta et al, ApJ 2013; Solar Phys. 2014), or even lower (Muhr et al., Solar Phys. 2014).

Coronal dimming – CME footprint

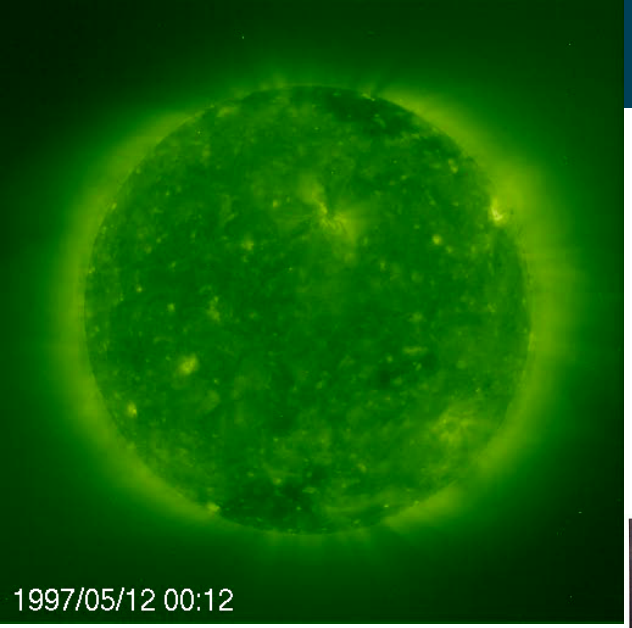

Classical twin dimmings

The coronal dimming signatures are caused by depletion of material emitting in EUV and some decrease of temperature (Hudson et al, 1996).

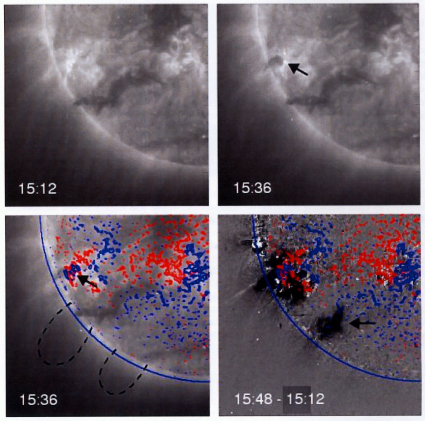

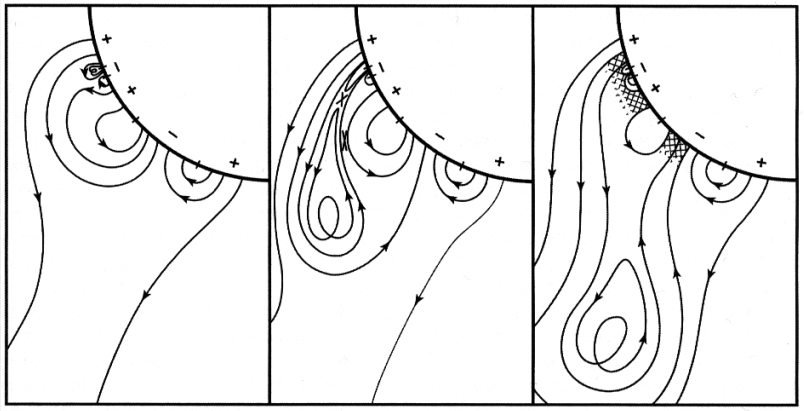

Moore & Sterling (2007): Distant dimming is produced by magnetic reconnection between adjacent magnetic arcades.

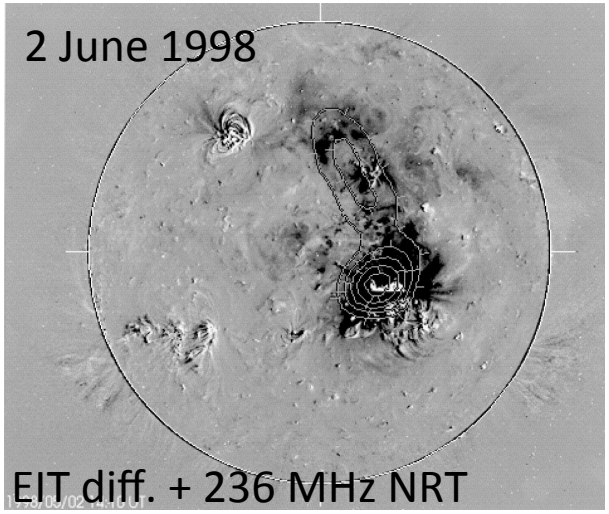

Transequatorial dimming overlayed by radio emission Pohjolainen et al. (2001)

The extent of coronal dimming indicates the lower-coronal extent of the coronal re-organisation caused by the CME.
Radio bursts indicate electron acceleration during the reconfiguration process.

CME-induced magnetic reorganisation in action

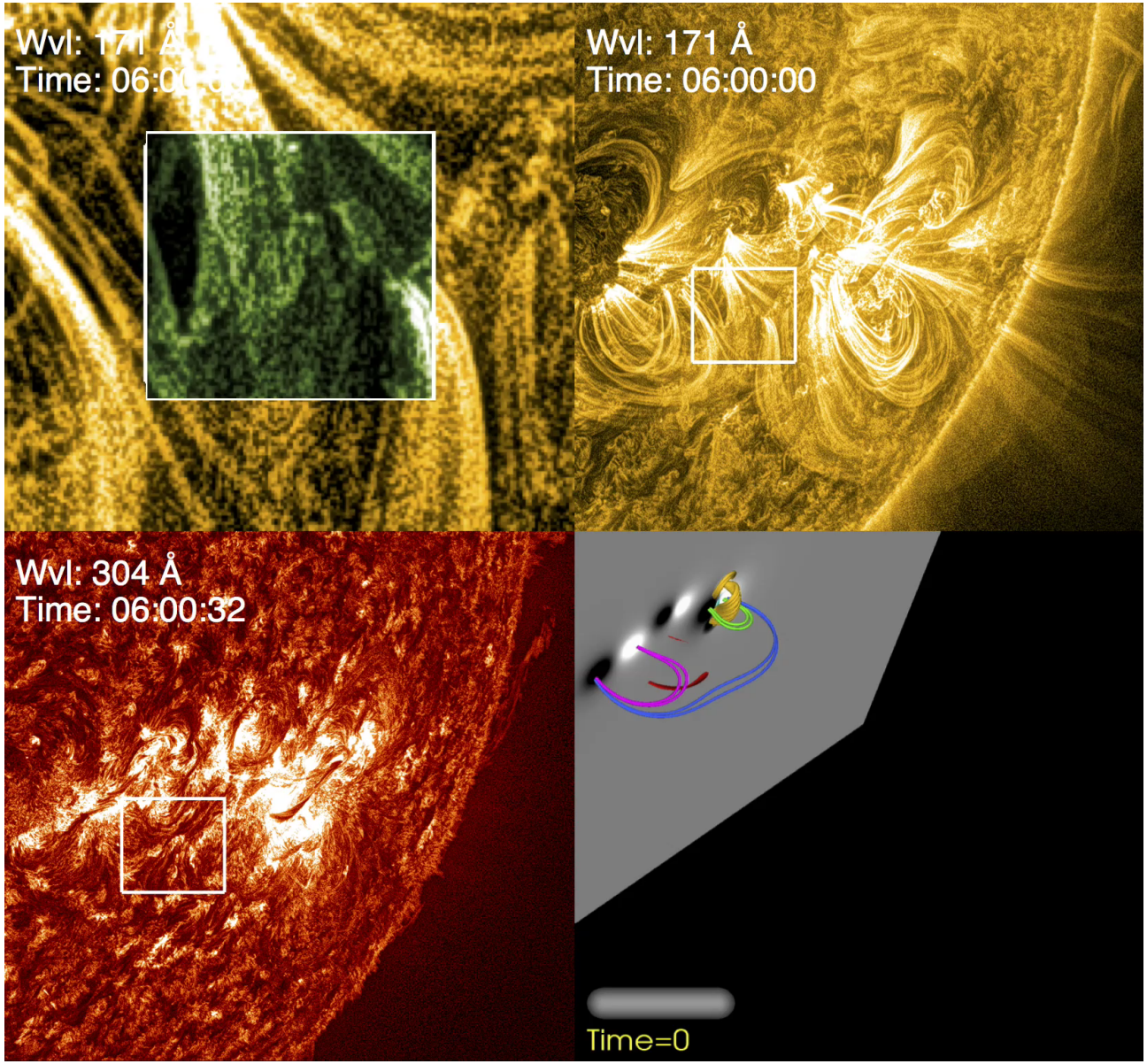

Reconnection between laterally expanding CME inducing reconnection with magnetic field of a neighbouring AR at 200 Mm distance.

AIA observations combined with data-constrained numerical MHD simulations of the event.

van Driel-Gesztelyi, *et al.,* ApJ, 788:85, 2014

Ground-based coronagraph observations

MLSO Mk3 observations on 22 Oct. 1989

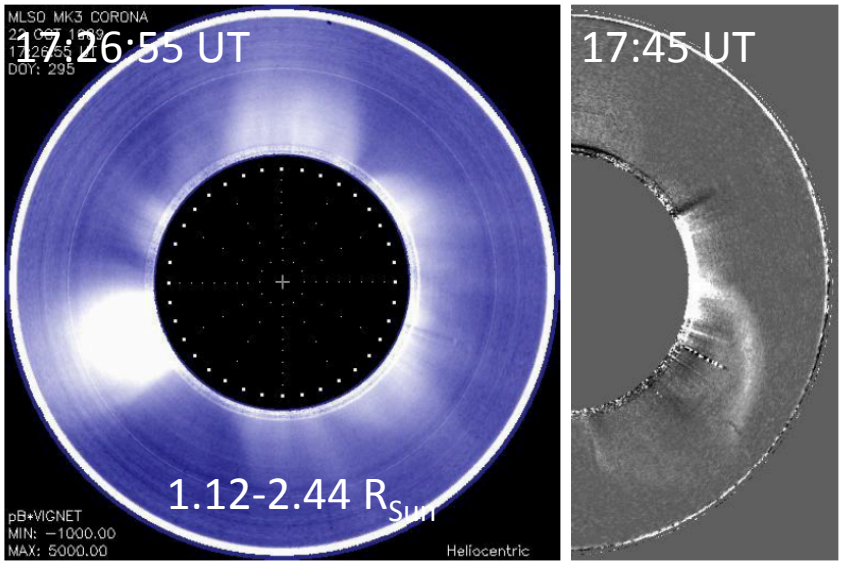

HAO A-013 18 Aug. 1980 10:04-13:34

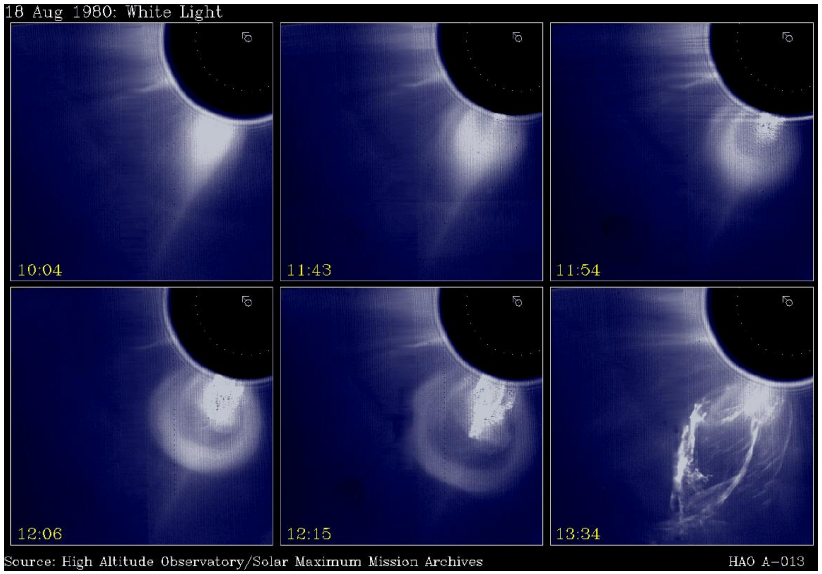

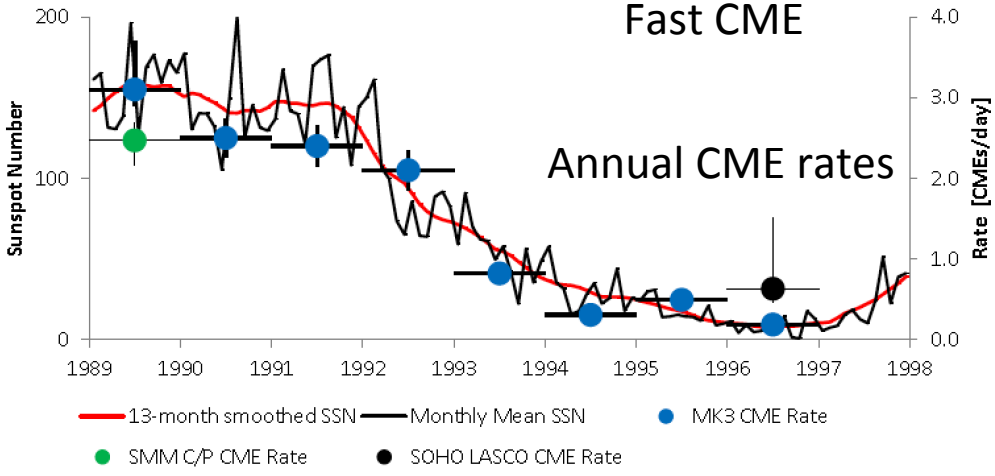

St.Cyr et al., Solar Phys. 2015

- Coronagraphs were invented ~80 years ago (Lyot, 1933) and have been used since to record CMEs.
- Since mid-1950s routine observations. Most recent: K-Cor (1.05-3 R_{sun}) de Wijn et al., 2012.

- **The long synoptic sequences of ground-based coronagraphs have their great value.**
- **Cover a height gap not observed with space-borne coronagraps.**

CME – space-borne coronagraph observations

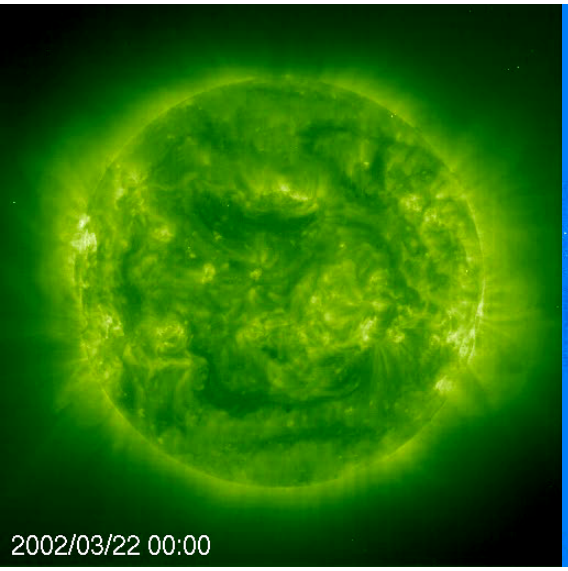

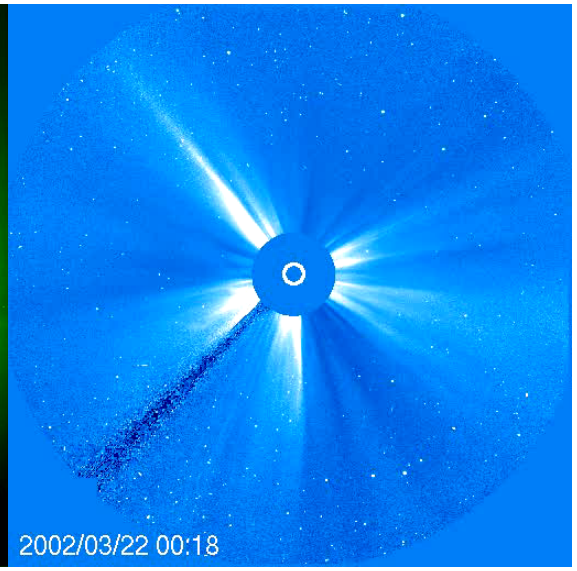

1st Space-borne CME observation: NRL-instrument on OSO-7 (Tousey, 1973)
Skylab, Helios, Solwind, and SMM
LASCO coronagraphs (Brueckner et al., 1995) since 1995.
STEREO SECCHI COR 1 & 2, HI since 2006/7 (STEREO-B – no contact since a year. Hope is still not lost, though. STEREO-A is back in contact.

Continuity of space-borne coronagraphs providing Earth-view (L1) and placed in L5 are needed.

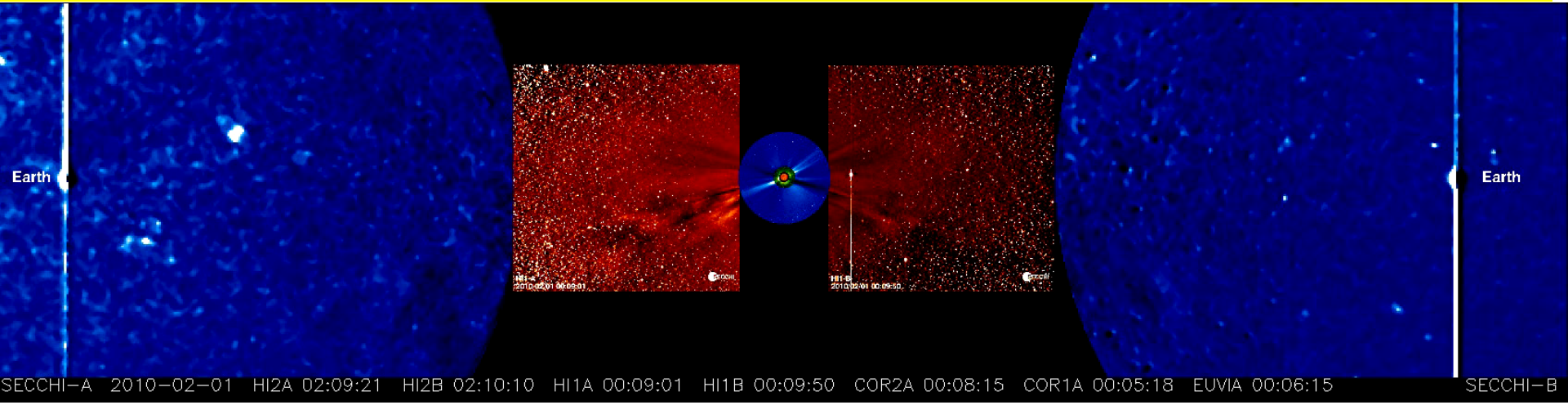

Combined observations: Energetics of CMEs

Emslie et al. (2012 ApJ 759, 71) evaluated all the above for 38 eruptive events between 02/2002-12/2006 the figure shows results for 6 events for which all energetic components were measured.

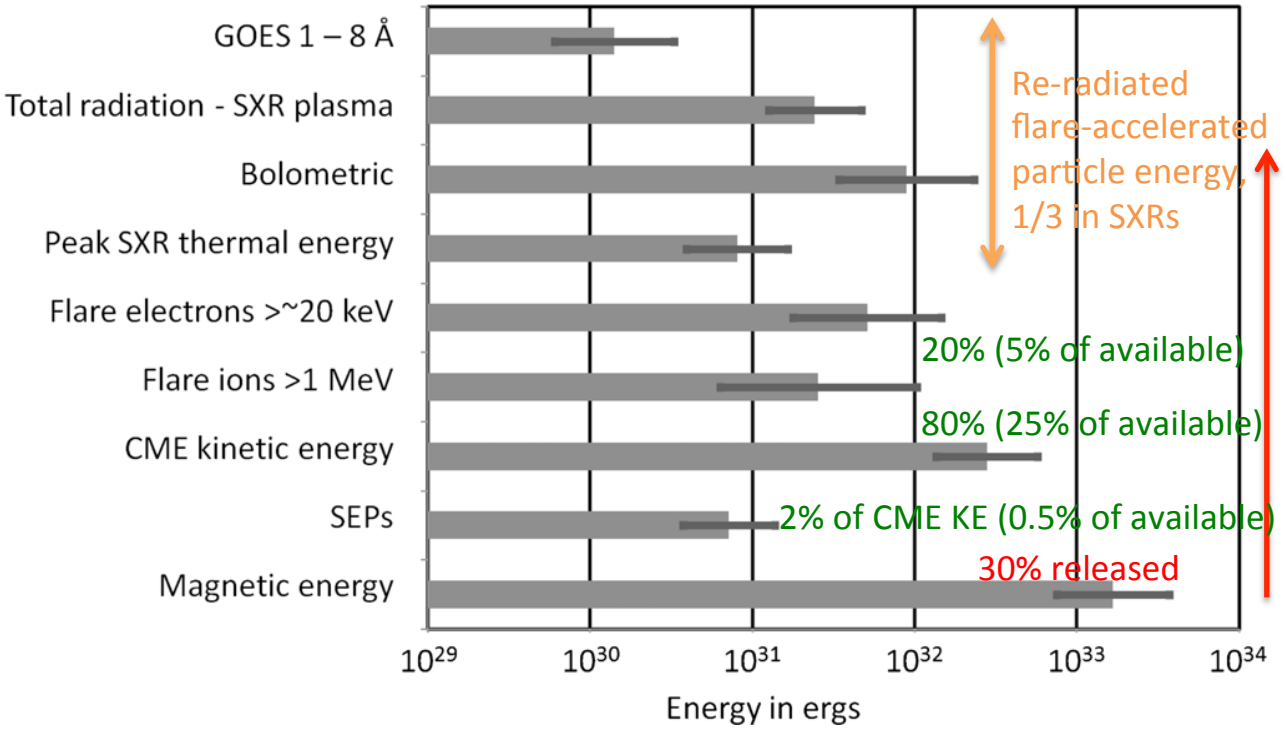

They concluded:

- the energy radiated by the SXR-emitting plasma exceeds, by about half an order of magnitude, the peak energy content of the thermal plasma that produces this radiation (suggesting continuous energy supply)
- the energy content in flare-accelerated electrons and ions is sufficient to supply the bolometric energy radiated across all wavelengths throughout the event (i.e. more than just the SXR emission)
- the energy contents of flare-accelerated electrons and ions are comparable (-> acceleration models)
- the energy in SEPs is typically a few percent of the CME kinetic energy (measured in the rest frame of the

Future improvements: DEM from Hinode/EIS, SDO/AIA & EVE; vector magnetograms from SDO/HMI + include turbulent mass motions+cumulative heating of CME plasma (Murphy et al., 2011) + 2nd flare phase (Woods et al., 2011; Su et al., 2012) + EIT wave (Long et al., 2015)

Global coronal wave energy

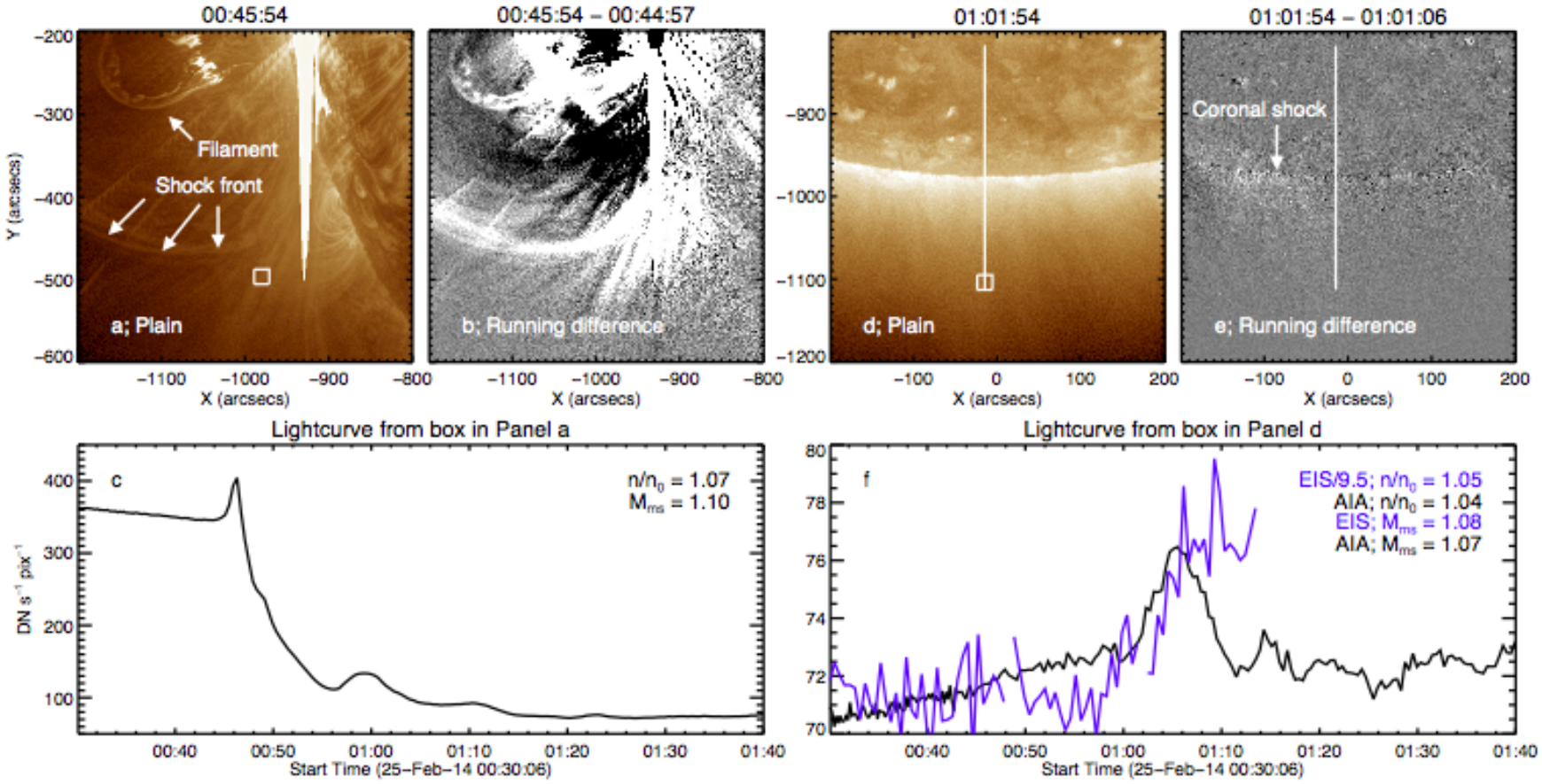

- Event from 25 Feb. 2014 with Type II burst and sharp front in EUV
- Intensity jumps close to source and at southern polar hole in both AIA and EIS
- Energy derived using Sedov-Taylor relation for blast wave through variable density medium ~6 x 10^{31} ergs
- Approx. 10% that of associated CME (~2.5 x 10^{32} ergs) (Long et al., ApJ 799:224, 2015)

Conclusions

- **The temperature** in the solar atmosphere **extends up to four orders of magnitude** during periods of **CME activity**.
- Consequently, the **wavelength**s we can observe certain details range **from radio, through optical to X-rays**. **Non-thermal effects** further broaden the range.
- Large transients show signatures at most wavelengths, which in turn **provide highly complementary information**, necessary for a **synthesis**.
- To form an increasingly complete observational picture of CMEs, **we need broad and ever-broadening multi-wavelength, multi-instrument observational coverage both from the ground and space**.
- As the **formation of CMEs involve long time-scales** and only probabilistic predictions are available for their onset time, we **need long synoptic sequences**.
- Once the **onset** is imminent, the sequence of events accelerates and there is a **need for high-cadence observations**.
- Even in the low corona, **CMEs couple small scales** (e.g. flare in their source active region) **and large scales** (e.g. the extent of a Moreton or global EUV wave).
- Therefore we **need high spatial resolution** observations focused on the small-scale, but should we neglect its **large-scale signatures** and its **interaction with surrounding magnetic fields**, we will never fully understand a CME.

The need for coordinated multi-wavelength observations from space and ground

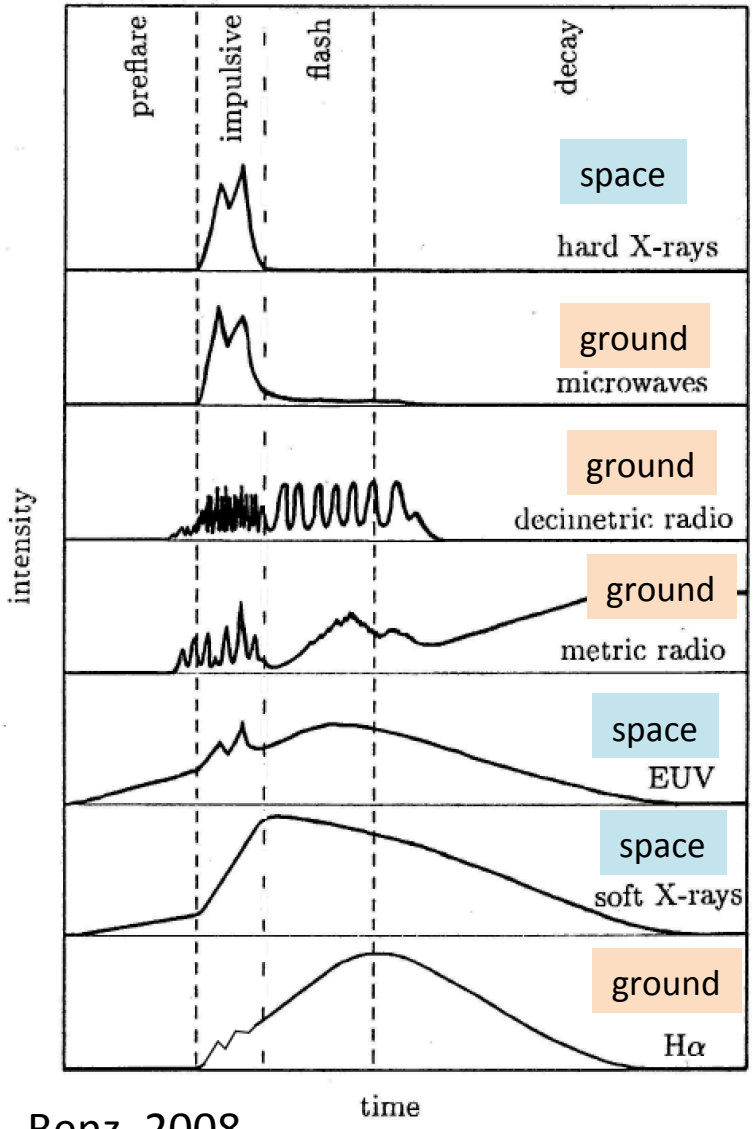

Benz, 2008

- Not a single facility/instrument can address alone the many varied scales and ranges of solar activity.

  time: decades *vs.* (sub)seconds

  spatial: full-disc *vs.* flaring kernel size

  wavelength: radio *vs.* γ-rays

=> Need to maintain an array of facilities/instruments.

- Much is to be learned from a *broad wavelength range* approach

⇒ Need for coordinated observations among various facilities from space and ground.